Applied Catalysis B: Environmental 87 (2009) 190–199

Contents lists available at ScienceDirect

Applied Catalysis B: Environmental

journal homepage: www.elsevier.com/locate/apcatb

Effects of oxidative modification of carbon surface on the adsorption of sulfur compounds in diesel fuel

Anning Zhou [a,b], Xiaoliang Ma [a], Chunshan Song [a,*]

[a] Clean Fuels and Catalysis Program, EMS Energy Institute, The Pennsylvania State University, 209 Academic Projects Building, University Park, PA 16802, USA
[b] Department of Chemistry and Chemical Engineering, Xian University of Science and Technology, Xian 710054, China

ARTICLE INFO

Article history:
Received 6 July 2008
Received in revised form 26 August 2008
Accepted 5 September 2008
Available online 5 October 2008

Keywords:
Oxidative modification
Carbon surface
Adsorption
Adsorptive desulfurization
Sulfur compounds
Diesel fuel
Activated carbon
Dibenzothiophene
Dimethyldibenzothiophene

ABSTRACT

This work examines the effects of modification of activated carbons (ACs) by HNO_3 oxidation and gas-phase O_2 oxidation, respectively, on the liquid-phase adsorption of sulfur compounds in diesel fuel. The adsorption characteristics of the oxidized and the original AC samples were evaluated in a fixed-bed flow system by using a model diesel fuel containing 400 parts per million by weight (ppmw) of sulfur as thiophenic compounds and 10 wt% of aromatics in a paraffinic solvent. The pore structure and surface properties of the AC samples were characterized by N_2 adsorption, SEM, FTIR, XPS and surface pH measurements. The adsorptive selectivity factor of the AC samples increases in the order of benzothiophene (BT) ≈ naphthalene (Nap) < 2-methyl naphthalene (2-MNap) < dibenzothiophene (DBT) < 4-methyldibenzothiophene (4-MDBT) < 4,6-dimethyldibenzothiophene (4,6-DMDBT). It was found that the HNO_3 oxidation was an efficient method in improvement of the adsorption performance of the AC for sulfur compounds. The improved adsorption performance upon the HNO_3 oxidation can be attributed mainly to an increase in the acidic oxygen-containing functional groups. However, the improved adsorption capacity upon oxidation is unlikely due to an increase in mesoporous or microporous surface/volume, although such attribution might have been inferred from the literature. An excellent correlation between the concentration of the surface oxygen-containing functional groups and the adsorption capacity per unit area as well as a good relationship between the adsorption capacity and the surface pH value were observed in this work, which suggest that the adsorption of the sulfur compounds over AC from the liquid hydrocarbon fuel may involve an interaction of the acidic oxygen-containing groups on AC with the sulfur compounds.

1. Introduction

Liquid-phase selective adsorption has recently become an important subject in ultra-deep desulfurization for ultra-clean fuels [1–6]. For environmental protection, the sulfur content in gasoline and diesel fuel needs to be reduced to less than 30 and 15 parts per million by weight (ppmw), respectively, according to US EPA regulation since 2006 [1–3]. On the other hand, for producing hydrogen from liquid hydrocarbon fuels, the sulfur content in the fuels needs to be reduced to less than 1 ppmw. Even the non-road liquid fuels need to comply with the low-sulfur regulations and further lower sulfur contents are expected in the future regulations worldwide [1,2,6]. All these requirements are promoting the research and development of new approaches for deep desulfurization of liquid hydrocarbon fuels, as the conventional desulfurization technology is difficult or costly to reduce the sulfur in the liquid hydrocarbon fuels, especially in diesel fuel, to the required low-ppmw level [1–9].

Adsorption desulfurization has become a promising approach in the ultra-deep desulfurization, because this approach shows some significant advantages, such as being able to reduce the sulfur to less than 1 ppmw and operating at ambient conditions without using H_2 [1,3,5]. A crucial issue in a successful adsorption process is to identify and develop a novel adsorbent, which has high adsorptive capacity, high selectivity and good regenerability [10–13]. Recently, significant attention has been paid to the carbon-based adsorbents for adsorptive desulfurization, because (1) these adsorbents usually have higher surface area, (2) their porous structure and surface chemical property can be modified easily, and (3) the sources for preparation of carbon-based adsorbents are wide and the production cost is relatively cheaper. For deep desulfurization of diesel fuel, another motivation for using carbon-based adsorbents is that some carbon material shows higher selectivity for removing the dibenzothiophenes (DBTs) with

* Corresponding author. Tel.: +1 814 863 4466.
E-mail address: csong@psu.edu (C. Song).

0926-3373/$ – see front matter © 2008 Elsevier B.V. All rights reserved.
doi:10.1016/j.apcatb.2008.09.024

one or two alkyl groups at the 4 and/or 6 positions [12,14]. These sulfur compounds are considered as the most refractory sulfur compounds in the diesel fuel, because they are very difficult to be removed by the conventional HDS technology or by the adsorption on other adsorbents due to the steric hindrance of the alkyl groups [6,12,14,15].

Both porous structure and surface chemistry of activated carbons (ACs) may play an important role in determining their adsorption performance. In a study on adsorption of polyaromatics such as phenanthrene vapor on the HNO_3-treated and H_2O_2-treated ACs, Garcia et al. [16] found that the higher the total number of surface oxygen groups, the lower the phenanthrene adsorption capacity. In a study of the adsorption desulfurization of DBT from a heptane solution on the H_2SO_4-modified AC, Jiang et al. found that the adsorption capacity of the H_2SO_4-modified AC for DBT was approximately two times of that on the unmodified AC [17]. They attributed this significant increase of the adsorption capacity to the increase in mesopore volume, although their experimental data also showed a significant increase in the number of oxygen containing function groups on the surface after the H_2SO_4 modification. For the removal of DBT from a n-hexadecane solution on the carbon aerogels, Haji and Erkey reported that the carbon aerogel with the larger average pore size had a higher sulfur adsorption rate and a higher capacity for DBT [18]. In study of structural and chemical heterogeneity of AC surfaces for adsorption of DBT, Ania and Bandosz found a linear correlation between the capacity and the volume of narrow micropores (<0.7 nm). They proposed that the higher uptake might be linked to the large volume of narrow micropores [19]. Recently, Ania et al. reported that the adsorption of DBT on AC is governed by both physisorption on the microporous network of the carbon and chemisorptions, and introduction of surface acidic groups enhanced the performance of the carbons for DBT [20]. However, Yu et al. reported that the HNO_3-modified AC improved the adsorption performance of AC for removal of thiophene, but degraded the adsorption performance of AC for removal of DBT [21]. It appears that the effect of the acid treatment on the adsorptive performance of AC for sulfur removal reported by different researchers is quite different, even discrepant with each other, and the mechanisms proposed are also quite different. Consequently, the fundamental understanding and clarification of the roles of pore structure and functional groups on the surface in the adsorptive desulfurization and the adsorption mechanism are crucial for design and development of a novel carbon-based adsorbent for deep desulfurization.

In our previous study on adsorptive desulfurization using a model diesel fuel with different thiophenic sulfur compounds and aromatics [12], we found that (1) the adsorptive capacity and selectivity of carbon materials are not simply dependent on the porous structure of adsorbents, (2) the surface chemistry of AC might play a more important role and (3) increase in the oxygen-containing functional groups on the surface appears to enhance sulfur–adsorption capacity.

Increase of the adsorption capacity and selectivity of the carbon-based adsorbents is crucial in the adsorptive desulfurization. As well known, both surface physical and chemical properties of AC can be modified by oxidation treatment, which is effective for enhancing the surface oxygen-containing groups on AC, and at the same time may change pore structure and area surface [22–26]. In order to improve the adsorption performance of AC for deep desulfurizaton of liquid hydrocarbon fuels, the oxidative modification of two commercial AC samples was conducted in the present study by using HNO_3 and O_2 as an oxidant, respectively. The modified AC samples were characterized by nitrogen adsorption, Fourier transform infrared spectroscopy (FTIR), surface pH measurement and X-ray photoelectron spectroscopy (XPS). The adsorption performance of the AC samples was evaluated in a flow system. Effects of porous structure and surface chemistry on the adsorption capacity and selectivity were examined. The roles of pore structure and the surface functional groups of AC in adsorptive desulfurization and the adsorption mechanism were discussed. It has been found that the oxidation modification improved the adsorption capacity by more than three times. It has become clear through this study that the improvement of the adsorptive performance by the HNO_3 oxidation modification is dominantly through an increase of the oxygen-containing functional groups, especially carboxyl groups, on the AC surface, but unlikely due to an increase in microporous surface/volume nor through an increase in the mesoporous surface/volume.

2. Experimental

2.1. Carbon materials

Two commercial ACs from Calgon and Westvaco, respectively, denoted by ACC and ACNU, were used in the present study. ACC is a typical microporous AC with surface area of 899 m^2/g, while ACNU is a typical mesoporous activated carbon with surface area of 1843 m^2/g. The AC samples were dried at 110 °C in a vacuum oven for 2 h before using for the tests.

2.2. Oxidative modification of ACs

2.2.1. Oxidation modification by nitric acid

Analysis-grade 68% nitric acid (EM Science) was used for oxidative modification of the ACs under mild conditions. The oxidation process was conducted by adding 30 ml of the nitric acid to 3 g of the AC sample placed in a glass conical flask with a magnetic stirrer. The mixture was kept at 60 °C for 3 h, and then, filtered to remove the solution. The treated AC sample was further washed with the distilled water until the filtrate became neutral. The filter cake was dried at 110 °C in a vacuum oven for 36 h, and then, kept in a glass bottle with a cover before use. The AC samples prepared from ACC and ACNU by the HNO_3 treatment were denoted as NO-ACC and NO-ACNU, respectively.

2.2.2. Oxidation modification by O_2

About 10 g of AC sample was placed in a stainless steel flow reactor. The reactor was heated to 350 or 400 °C at a heating rate of 5 °C/min under a N_2 flow, and then, the reactor was kept at this temperature under a flow of 5 vol.% O_2 in N_2 for 3 h. After the oxidation, the reactor was cooled to the room temperature, and the oxidized ACC and ACNU were kept respectively in a glass bottle before use. The oxidized product from ACC at 400 °C for 3 h was denoted as O-ACC and that from ACNU at 350 °C for 3 h was denoted as O-ACNU.

2.3. Model diesel fuel

A model diesel fuel (MDF) was made by adding model sulfur compounds and aromatic compounds into a paraffin solvent. MDF contained benzothiophene (BT), dibenzothiophene (DBT), 4-methyldibenzothiophene (4-MDBT) and 4,6-dimethyldibenzothiophene (4,6-DMDBT) with the same molar concentration (3.0 mmol/kg). In order to examine the adsorptive selectivity, the same molar concentration of naphthalene (Nap) and 2-methylnaphthalene (2-MNap) were also added into MDF. MDF also contained 10 wt% of tert-butylbenzene to mimic the aromatic content in diesel fuel. The total sulfur content in MDF was 400 ppmw. The detailed composition of MDF is shown in Table 1.

2.4. Characterization of ACs

2.4.1. Porous structure

The porous structure of the AC samples was characterized by adsorption/desorption of nitrogen at 77 K using Micromeritics ASP2010 surface area and porosimetry analyzer. Standard BET and DR model were applied respectively to derive surface area and pore volume. The pore size distribution was calculated according to BJH model. Scanning electron microscopy (SEM) analysis of ACNU and NO-ACNU samples were conducted by using Hitachi model S-3500N instrument.

2.4.2. X-ray photoelectron spectroscopy (XPS)

The elements and surface functional groups on the AC sample were analyzed by X-ray photoelectron spectroscopy (XPS). XPS analysis was carried out under high vacuum of $<10^{-9}$ Torr, using pass energy 80 eV for surveys and 20 eV for chemical state with the Kratos Analytical Axis Ultra instrument (X-ray source Monochromatic aluminum, 1486.6 eV, take off angle: 90° with respect to sample plane). The analyzer magnification was hydrid, 700 μm × 250 μm. The peak positions were corrected on the basis of the most intense graphitic carbon peak, which is taken as 284.3 eV (for C 1s). The samples were pressed in a mortar and pestle into 3 M double-sided tape and mounted on conducting carbon tape. Optical viewing at 20× in a stereomicroscope indicated a uniform and continuous coverage of the sample powders. XPS quantification was performed by applying the appropriate relative sensitivity factors (RSFs) for the Kratos instrument to the integrated peak areas. These RSFs take into consideration of the X-ray cross-section and the transmission function of the spectrometer. The approximate sampling depth under these conditions is 50 Å. A survey scan was initially recorded for the sample to identify elements present. The composition of the sample powder surfaces was determined from the survey scans. Chemical states of O, N and C species were determined from the charge corrected hi-resolution scans. The C 1s peaks for the samples were curve fit with 5 peaks representing C-graphite, C-graphite*, CO, COO, and CO_3 [12,25,27]. C-graphite peak arises from aromatic layers in graphitic sp^2 configurations, while the C-graphite* peak arises from regions of defective structures, exhibiting a more or less pronounced sp^3 character.

2.4.3. FTIR analysis

In order to qualitatively analyze the functional groups on the surface, the FTIT analysis of some AC samples were carried out by using Nicolet Nexus 670 spectrometer within the range of 600–4000 cm^{-1}. The AC samples were dried in an oven at 110 °C for overnight before the FTIR analysis. Specimen of the AC was first mixed with KBr at a sample/KBr weight ratio of 1/200, ground in an agate mortar, and then the mixture was pressed at 10 tonnes for 5 min. The 64 scans and 4 cm^{-1} resolutions were applied in recording the spectra. The background of pure KBr was automatically subtracted from the sample spectrum.

2.4.4. Measurement of surface pH

A sample of 0.5 g of AC was added to 25 ml of water. The suspension was stirred for 24 h to reach equilibrium. Then, the AC sample was filtered and the pH of solution was measured by Orion pH meter. This is an indirect measure of surface pH and the value is good for comparison only for the measurement under the same conditions.

2.5. Adsorption experiments

Adsorptive desulfurization of MDF over the AC samples was conducted in a fixed-bed flowing system with a stainless steel column (length: 15 mm, diameter: 4.6 mm). About 1.0–1.6 g of the AC sample, which was dried at 110 °C in a vacuum oven for 2 h before test, was packed into the column. MDF was then fed into the column from the bottom by a HPLC pump. The adsorption conditions were controlled at a liquid hourly speed velocity (LHSV) of 4.8 h^{-1} and a temperature of 25 °C. The treated fuels were periodically sampled at an interval of 15–20 min for analysis.

In order to facilitate the quantitative analysis and discussion of the adsorptive performance of AC samples, a breakthrough capacity and a relative selectivity factor for each compound were used in the present study. The breakthrough capacity was calculated by equation shown below:

$$\mathrm{Cap}_{\mathrm{total}} = W_{\mathrm{total}} \times \frac{C_0}{W_{\mathrm{ads}}} \quad (1)$$

where W_{total} is the breakthrough weight of the treated fuel, C_0 is the initial concentration of sulfur in the fuel and W_{ads} is the weight of the adsorbent tested. The breakthrough sulfur level was 0.5 ppmw, which was the limitation of the total sulfur analyzer used in the present study. The relative selectivity factor was defined as:

$$\alpha_{i-n} = \frac{\mathrm{Cap}_i}{\mathrm{Cap}_n} \quad (2)$$

where Cap_i is the breakthrough capacity of compound i, and Cap_n is the breakthrough capacity of the reference compound, Nap.

2.6. Analysis of the treated MDF samples

The total sulfur concentration of the treated fuel samples was analyzed by using ANTEK 9000 series sulfur analyzer. The detailed analysis method was reported in our previous paper [28]. The concentration of various compounds in the treated MDF was quantitatively analyzed by a HP 5890 gas chromatograph with a capillary column (XTI-5 phase, Restek, 30 m in length, 0.25 mm in internal diameter) and a flame ionization detector (FID), using n-tetradecane as an internal standard.

3. Results and discussion

3.1. Effect of oxidative modification on texture structure of ACs

Nitrogen adsorption–desorption isotherms of ACC, ACNU, modified ACC and modified ACNU are shown in Fig. 1. All nitrogen adsorption isotherms are of type I according to the classification by Brunauer et al. [29]. The N_2 adsorption capacity on the ACs increased in the order of NO-ACNU < NO-ACC ≈ ACC < O-ACNU and < ACNU. A hysteresis loop was observed at the relative high pressure for O-ACNU and ACNU, indicating the presence of mesopores, which can also be found from the BJH mesopores size distribution of the ACs, as shown in Fig. 2. The significantly higher slope of O-ACNU and ACNU also suggests the textural heterogeneities. The estimated texture parameters on the basis of the nitrogen adsorption–desorption isotherms are summarized in Table 2. ACC was a microporous AC with $S_{\mathrm{mic}}/S_{\mathrm{meso}}$ ratio of 3.7, while the ACNU was a mesoporous AC with $S_{\mathrm{mic}}/S_{\mathrm{meso}}$ ratio of 0.1. The HNO_3 oxidation only slightly changed the texture structure of ACC. However, the HNO_3 oxidation significantly changed the texture structure of ACNU. S_{BET} decreased from 1843 m^2/g for ACNU to 488 m^2/g for NO-ACNU, leading to about 74% loss of the total surface area, whereas S_{mic} increased from 178 to 301 m^2/g by about 70% after the oxidation, although the average pore size was almost the same (2.9 nm). It was found that the HNO_3 oxidation not only changed the total surface area and pore distribution, but also changed the surface morphology of ACNU, as

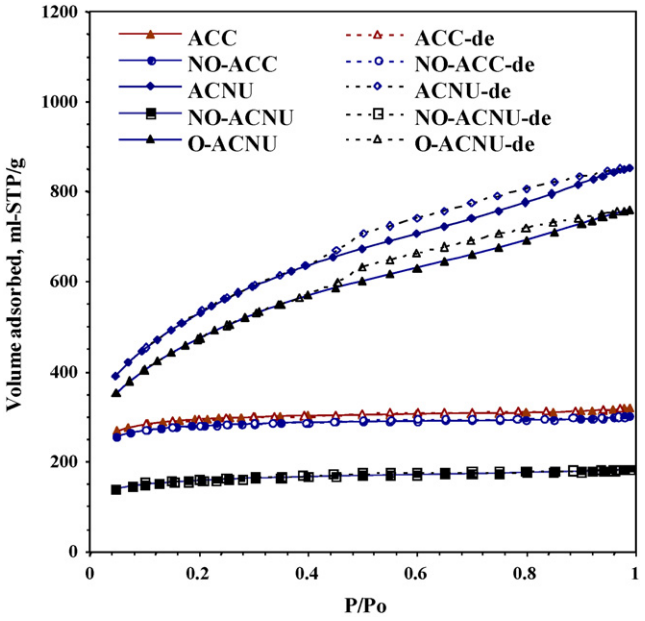

Fig. 1. Effect of the oxidation modification on N_2 adsorption–desorption isotherms of ACs at 77 K.

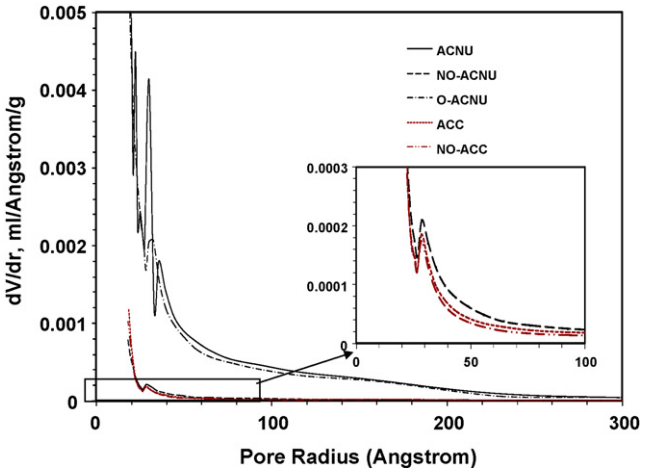

Fig. 2. Effect of the oxidation modification on the pore distributions of ACs.

shown by the SEM micrographs of ACNU and NO-ACNU in Fig. 3. It clearly shows that the HNO_3 oxidation resulted in the surface erosion, the increase of the surface roughness and some particle disintegration of ACNU.

Table 1
Composition of model diesel fuel (MDF).

Name	Purity	Conc. wt%	mmol/kg	S. conc. ppmw
BT	0.99	0.0418	3.084	99.9
DBT	0.98	0.0575	3.058	100.1
4-MDBT	0.96	0.0618	2.992	100.0
4,6-DMDBT	0.97	0.0662	3.024	100.0
Nap	0.99	0.04	3.090	
2-Map	0.97	0.0443	3.022	
n-Decane	0.99	44.31		
n-Hexadecane	0.99	44.31		
n-Tetradecane	0.99	0.059	(Internal standard)	
tert-Butylbenzene	0.99	10.00		
Others		1.0		

The significant reduction of the surface area of ACNU in the HNO_3 treatment oxidation is likely due to the partial destruction of the pore structure by the oxidation, which also led to the generation of oxygen functional groups. ACC was produced from coconut by steam activation and ACNU was prepared from wood by chemical activation (H_3PO_3). The significant difference in the effect of the HNO_3 modification on the texture structure of ACC and ACNU indicates that the change of porous structure by the HNO_3 modification also depends on the precursor of ACs and/or the activation method, as also reported by El-Hendawy [23].

Different from the effect of the HNO_3 oxidation, the O_2 oxidation of ACNU at 350 °C only slightly changed the porous structure. S_{meso} decreased by about 13% and S_{mic} was almost no change after the O_2 oxidative modification, indicating that the texture structure of ACNU is more resistant to the O_2 oxidation than to the HNO_3 oxidation.

3.2. Effect of oxidative modification on surface chemistry of ACs

3.2.1. XPS characterization

The concentration of elements on surface of the studied ACs was detected by XPS and the results are listed in Table 3. The major elements on the AC surface are C and O. The C concentration on the surface of ACC and ACNU were similar, being 90.6 and 90.1 at.%, respectively. The O concentration (8.2 at.%) on the surface of ACNU was slight higher that of ACC (7.2 at.%). In addition of C and O, ACC contained some alkali ions, 0.3 at.% of Na^+ and 1.5 at.% of K^+. ACNU contained 0.4 at.% of Na^+ and 1.0 at.% of P, probably due to the chemical activation of ACNU by H_3PO_3 in production. It was found that the oxidation of the ACs, especially by the HNO_3 oxidation, increased the O concentration on the surface significantly. The O concentration increased by 92% and 157%, respectively, for ACC and ACNU after the HNO_3 oxidation, suggesting a huge increase of the oxygen functionalities on the surface. The HNO_3 oxidation also

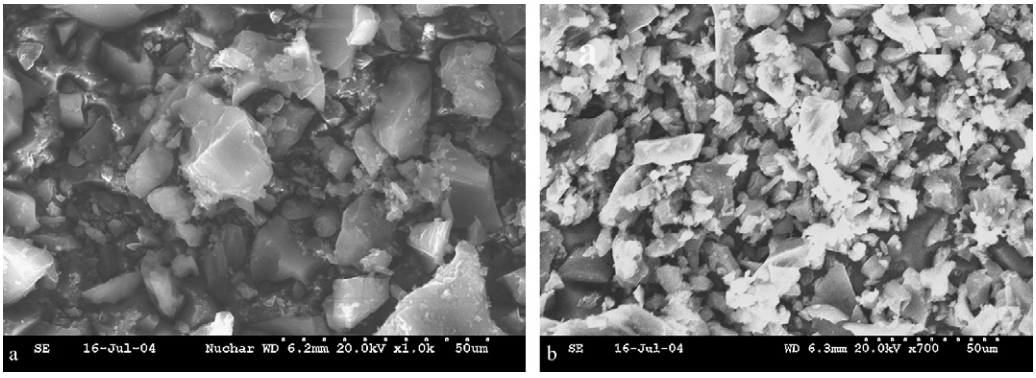

Fig. 3. SEM micrographs of ACNU (a) and NO-ACNU (b).

Table 2
Porosity parameters of ACs.

Sample	Description	S_{BET} ($m^2\,g^{-1}$)	S_{micro} ($m^2\,g^{-1}$)	S_{meso} ($m^2\,g^{-1}$)	S_{mic}/S_{meso}	V_{total} ($cm^3\,g^{-1}$)	V_{micro} ($cm^3\,g^{-1}$)	V_{meso} ($cm^3\,g^{-1}$)	Average pore size (nm)
ACC	PCB-G, Calgon	899	709	190	3.7	0.492	0.368	0.124	2.2
NO-ACC	Treated ACC by 69% HNO_3, 60 °C, 3 h	857	680	178	3.8	0.466	0.351	0.115	2.7
ACNU	Nuchar SA 20, Westvaco	1843	178	1666	0.1	0.990	0.085	0.904	2.9
NO-ACNU	Treated ACNU by 69% HNO_3, 60 °C, 3 h	488	301	187	1.6	0.282	0.159	0.124	2.9
O-ACNU	Treated ACNU by 5% O_2 in N_2, 350 °C, 3 h	1635	179	1457	0.1	1.172	0.091	1.080	2.9

Table 3
Concentration of elements on the surface of ACs on the basis of XPS analysis (at.% based on total atom number except hydrogen).

Sample	Na	O	K	C	Cl	N	Si	P
ACC	0.3	7.2	1.5	90.6	0.3	0.0	0.2	0.0
NO-ACC	0.0	13.8	0.0	84.8	0.1	0.9	0.3	0.0
ACNU	0.4	8.2	0.0	90.1	0.0	0.0	0.2	1.0
NO-ACNU	0.0	21.1	0.0	75.9	0.0	1.9	0.3	0.4
O-ACNU	0.5	8.8	0.0	89.2	0.0	0.0	0.0	1.3

Table 4
Concentration of different carbon and oxygen components in relative at.%.

Sample	C-graphite	C-graphite*	C–O	COO	CO_3	O–C (calc)	O–C (est)
ACC	65.3	16.1	3.2	1.4	4.5	6.1	5.9
NO-ACC	65.0	12.6	3.3	3.1	0.9	9.4	11.4
ACNU	76.5	10.3	1.9	1.0	0.5	3.9	5.2
NO-ACNU	58.1	9.4	3.7	4.7	0.0	13.1	15.7
O-ACNU	74.7	10.1	2.9	1.5	0.0	6.0	5.2

introduced some N-contained function group to the surface, as proved by the increase in nitrogen concentration on the surface. On the other hand, it was observed that the HNO_3 oxidation removed the Na^+ and K^+ ions from the AC, as these ions can be solved in the HNO_3 solution. The O_2 oxidation at 350 °C for 3 h only increased the O concentration on the surface of ACNU by about 7%. By comparison of the two oxidative methods, it is obvious that the HNO_3 oxidation is more efficient for increasing the oxygen functional groups on the ACNU surface.

The concentration of different carbon components (CO, COO and CO_3) and oxygen component (O–C) on the AC surface was estimated by XPS. The results are listed in Table 4. The HNO_3 oxidation of ACC significantly enhanced the concentration of COO group from 1.4 at.% for ACC to 3.1 at.% for NO-ACC, although no significant change in C-graphite and CO concentration was found, indicating that the HNO_3 oxidation might introduce some carboxyl group to the AC surface. Interestingly, the HNO_3 oxidation reduced the concentration of CO_3 from 4.5 at.% for ACC to 0.9 at.% for NO-ACC, probably due to the removal of carbonate existing in ACC in the HNO_3 oxidation treatment. It is in agreement with the removal of K^+ and Na^+, which could be present in AC in the form of K_2CO_3 and Na_2CO_3. For ACNU, the HNO_3 oxidation not only increased the concentration of COO significantly, but also enhanced the concentration of CO. Moreover, the HNO_3 oxidation reduced the concentration of C-graphite on ACNU surface significantly (from 76.5 to 58.1 at.%), but the similar result was not observed for the HNO_3 oxidation of ACC. It indicates that (1) the HNO_3 oxidation destroys partly the skeleton structure of ACNU and (2) the extent of such destroying depends the structure of AC. These results are consistent with the effect of the HNO_3 oxidation on the porous structure discussed above. However, the O_2 oxidation increased the concentration of CO more significantly than that of COO, implying that the O_2 oxidation may prefer to produce C═O groups in comparison with the HNO_3 oxidation.

3.2.2. FTIR analysis

Fig. 4a shows FTIR spectra of ACC and NO-ACC. The absorption bands in the range of 3000–3600 cm^{-1} can be ascribed to stretching vibration of hydroxyl groups (O–H), involved in hydrogen bonding and/or water adsorption on the carbons. The bands in the range of 1850–1400 cm^{-1} are mainly absorption bands of C═O, C–N– and aromatic ring. There are two major characteristic peaks in this band, as shown in Fig. 4a. The little peak centered at 1720 cm^{-1} can be a contribution from the stretching vibrations of carboxyl groups (C═O) on the edges of layer planes or from conjugated groups in the lactone groups [23,30–32]. The peak at 1550 cm^{-1} and the shoulder peak around 1350 cm^{-1} can be

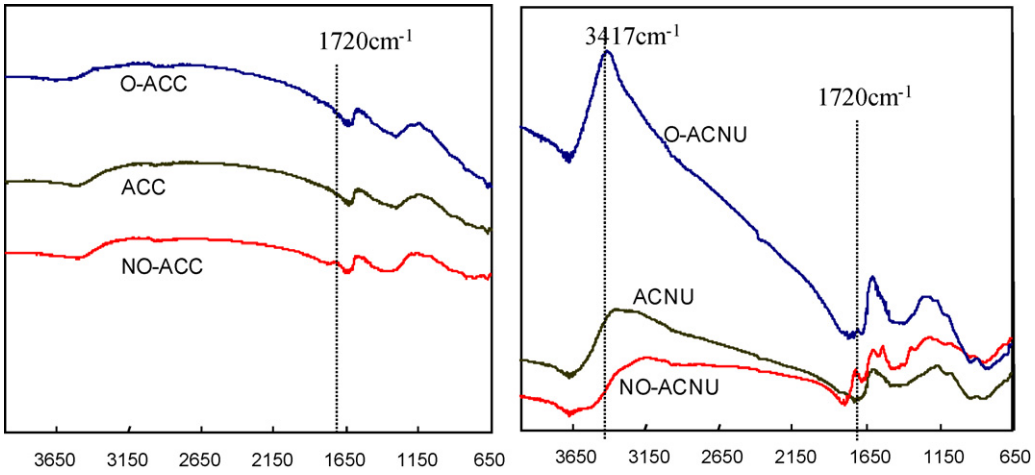

Fig. 4. FTIR spectra of ACs (a) ACC and oxidized ACC and (b) ACNU and oxidized ACNU.

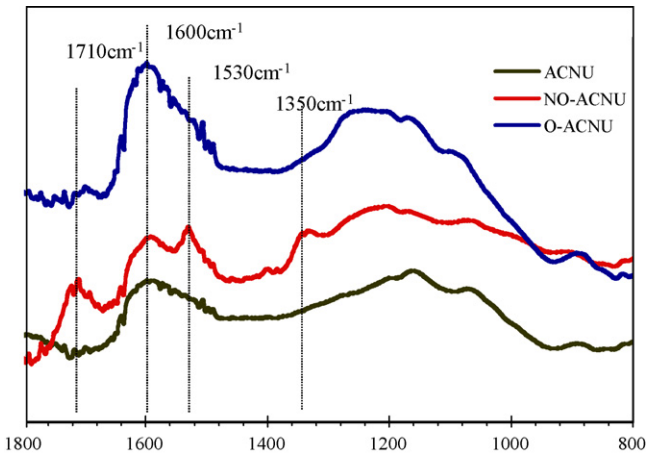

Fig. 5. FTIR spectra of ACs (ACNU and oxidized ACNU).

assigned to asymmertric and symmetric COO^- vibrations, respectively. The peak around 1150 cm^{-1} can be ascribed to the both C–O stretching and O–H bending modes in phenolic and carboxylic groups. It was observed that the HNO_3 oxidation enhanced the absorption intensity at 1720, 1550 and 1150 cm^{-1}, indicating an increase in carboxyl, lactone, and hydroxyl groups.

Figs. 4b and 5 show FTIR spectra of ACNU and the oxidized ACNU samples. There is significant difference between the samples from ACC and the samples from ACNU: (1) a stronger absorption at the band around 3400 cm^{-1} for the stretching vibration of hydroxyl groups for ACNU samples than for ACC samples and (2) a higher peak around 1600 cm^{-1}, which could be ascribed to the stretching vibrations of carboxyl groups (C═O) in the carbonate groups [25], was found for the ACNU samples. Another possibility for the contribution to the 1600 cm^{-1} band is the C═O group highly conjugate with the aromatic ring such as quinones. The HNO_3 oxidation enhanced significantly the absorption intensity at 1720, 1600, and 1550 cm^{-1}, indicating a significant increase in carboxyl, lactone, and hydroxyl groups on the surface of NO-ACNU. The broad absorption within the range between 1300 and 1000 cm^{-1} can be assigned to various C–O bonds. A significant increase of the absorption in this range suggests an enhancement of ethers, phenols and/or hydroxyl groups on NO-ACNU surface, which is in agreement with the increase in C–O number observed in the XPS analysis (see Table 4). It has been reported that the changes in the intensity of this bands upon treatment with HNO_3 are due to the formations of various oxygen surface groups and of structure containing N–O bonds (nitro groups and nitrate complexes) [23], which is also in agreement with the increase of N element observed in the XPS characteristics (see Table 3). These results are consistent with the previous findings that the AC oxidized by HNO_3 gave rise to a greater increase in C═O bonds in carboxyl acid and lactone groups among of carboxyl, carbonyl, and phenolic groups [33], in addition of nitro groups and nitrate complexes.

In comparison between ACNU and O-ACNU, it was found that the O_2 oxidation enhanced strongly the absorption around 3400 cm^{-1}, indicating a huge increase of the hydroxyl groups (O–H) on the surface of O-ACNU. The O_2 oxidation also significantly enhanced the absorption at 1600 cm^{-1} band, but not at the 1720 and 890 cm^{-1} bands. The results imply that the O_2 oxidation might increase the conjugated C═O groups, but not carboxyl groups, which is in agreement with observation from the XPS analysis that the increase in the CO concentration was higher than that in the COO concentration.

Table 5
Acidity and adsorptive capacity of ACs.

Sample	Acidity pH	Breakthrough capacity mg-S/g-AC	Breakthrough capacity μg-S/m^2
ACC	10.2	6.4	7.2
NO-ACC	3.9	11.3	13.1
O-ACC	10.1	4.9	5.1
ACNU	6.5	3.8	2.0
NO-ACNU	3.8	11.6	23.8
O-ACNU	4.2	5.1	3.1

3.2.3. pH value of ACs

pH values of ACC, ACNU and their oxidized products were measured. The results are listed in Table 5. The alkalinity of ACC was much higher than that of ACNU. In addition to the different functional groups on the surface, one of major reason for the higher alkalinity of ACC is probably that ACC contained much higher K^+-contained inorganic compound, such as K_2CO_3, as suggested by the XPS characterization data (Tables 3 and 4). It was observed that the HNO_3 treatment substantially increased the acidity of both ACC and ACNU, regardless their different texture structure. The pH value changed from 10.2 to 3.9 for ACC and from 6.5 to 3.8 for ACNU. The increase in the acidity of the ACs can be ascribed to both the removal of the basic inorganic compounds from the ACs and the introduction of the new acidic functional groups to the surface of the ACs. The former is supported by the removal of K^+ and Na^+ from the surface of ACs, as shown in Table 3, whereas the latter is reflected by the increase in the COO concentration on the surface, as shown in Table 4, and the increase of the infrared absorption corresponding to carboxyl and phenol groups, as shown in Figs. 4 and 5.

For the O_2 oxidation of ACC, it was found that the O_2 treatment only slightly changed the pH value for ACC. It is probably because (1) the O_2 treatment failed to remove the basic inorganic compounds in the sample, and (2) the increase of the acidic groups by the O_2 treatment is limited. For the O_2 oxidation of ACNU, the O_2 treatment at 350 °C decreased the pH value from 6.5 to 4.2, indicating a significant increase of the acidic functionality. The effect of the oxidation temperature on the pH value of the ACs was also examined. Interestingly, it was found that in a temperature range less than 350 °C, increase in the O_2 oxidation temperature favored the increase in the surface acidity of the ACs, while the surface acidity of the AC at 450 °C O_2 treatment was less than that at 350 °C. It indicates that the O_2 treatment at higher temperature might favor to introduce the basic functional group, such as ketone groups, to the surface instead of the carboxyl and phenol groups. The higher temperature will also result in the decomposition of the carboxyl groups.

3.3. Effect of oxidative modification on adsorption performance of ACs

3.3.1. Effect on adsorption capacity

Adsorptive desulfurization of MDF over ACC, ACNU and the modified ACC and ACNU was conducted at room temperature (25 °C) in the flow system. The breakthrough curves for ACNU, O-ACNU and NO-ACNU are shown in Fig. 6. The breakthrough capacity was calculated on the basis of the breakthrough curves and the results are listed in Table 5. The shapes of the breakthrough curves for ACNU, O-ACNU and NO-ACNU are similar to each other. However, the corresponding breakthrough volume is quite different. It is found that there are three jumps for each curve. The GC-FID analysis of the treated MDF samples indicates that the first jump corresponds to the breakthrough of BT, the second jump to the breakthrough of DBT and 4-MDBT, and the third jump to the breakthrough of 4,6-DMDBT, as reported before [12]. The O_2

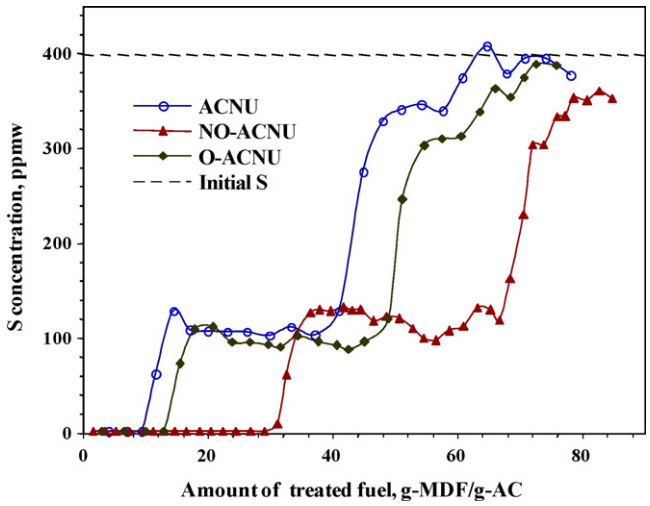

Fig. 6. Breakthrough curves for ACNU and oxidized ACNU.

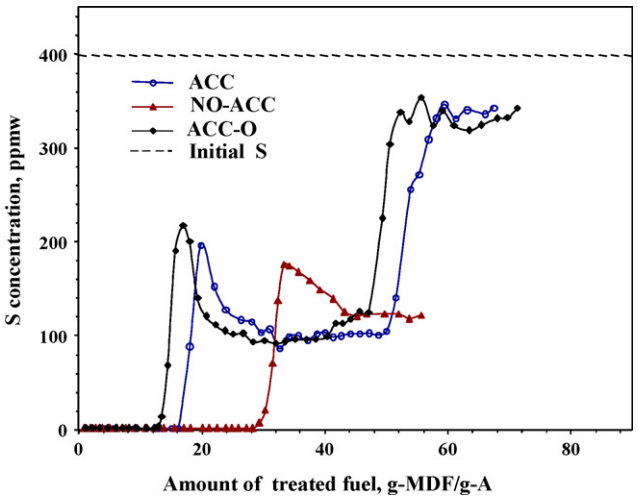

Fig. 7. Breakthrough curves for ACC and oxidized ACC.

oxidation increased the capacity from 3.6 mg-S/g-AC for ACNU to 4.9 mg-S/g-AC for O-ACNU by a factor of 1.4, while the HNO_3 oxidation increased the capacity to 11.1 mg-S/g-AC, about three times higher than that of ACNU. The result is different from the report by Yu et al., who found a negative effect of HNO_3 oxidation modification on the DBT removal performance of the AC [21]. This is probably due to much severer condition (120 °C for 5 h) that they used for the oxidation modification than that in the present study (60 °C for 3 h). The severe condition for the oxidation modification may result in the destruction of the pore structure of AC and thus decrease the surface area significantly, as also found in the present study (see Table 2). Another possibility is that the severe condition may introduce too many polar function groups onto the surface, which causes too strong hydrophilic property of the surface to adsorb the organic sulfur compounds.

The breakthrough curves for ACC, O-ACC and NO-ACC are shown in Fig. 7, and the corresponding breakthrough capacity values are also listed in Table 5. The HNO_3 oxidation increased the capacity from 6.4 mg-S/g-AC for ACC to 11.3 mg-S/g-AC for NO-ACC by about two times. However, the breakthrough capacity for O-ACC was only 5.1 mg-S/g-AC, indicating that the O_2 oxidation at 400 °C did not improve the adsorption performance of ACC, but had a negative effect. For all ACs tested, the breakthrough capacity increased in the order of ACNH < O-ACNU < O-ACC < ACC < NO-ACC < NO-ACNU.

In order to examine the effect of pore structure on the adsorption performance, the surface areas and pore volumes of ACs versus their adsorption capacities are shown in Fig. 8. It is clear that the adsorption capacity is neither a simple function of total surface area, microporous surface area or mesoporous surface area, nor a simple function of micropore volume and mesopore volume.

According to our previous study [12], the adsorption of sulfur compounds on AC obeys the Langmuir isotherm. Thus, the relative affinity (RA) of adsorbent can be expressed by:

$$\mathrm{RA} = K q_m = K Q_m S \quad (3)$$

where K is the adsorption equilibrium constant; q_m is the maximum adsorption capacity corresponding to the saturation coverage of the surface; Q_m ($Q_m = q_m/S$) is the maximum density of adsorption sites per unit area and S is the approachable surface. This equation indicates that the relative affinity of the adsorbent is not only directly proportional to the surface area (S), but also to the

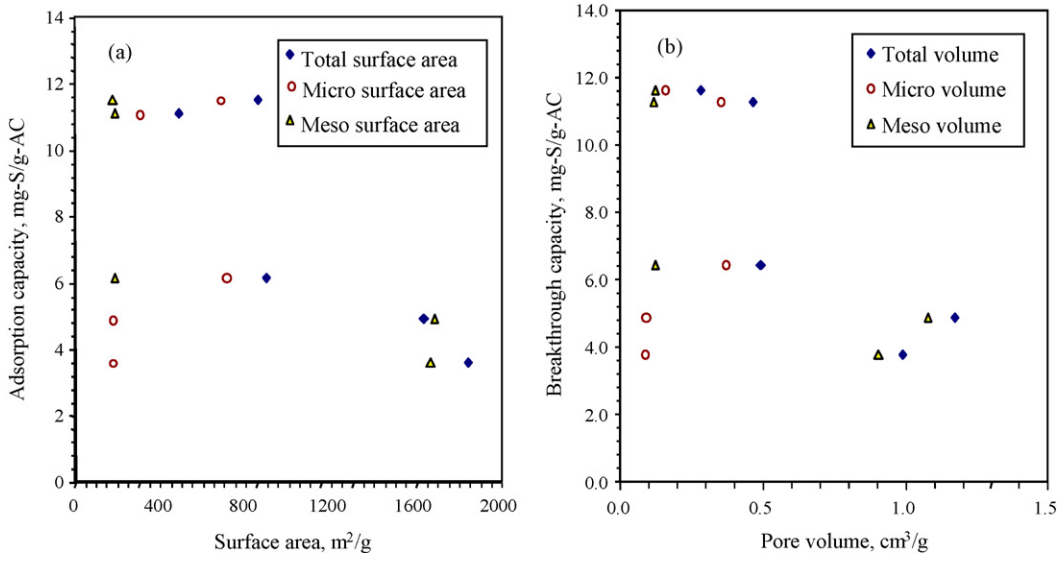

Fig. 8. Adsorption capacity versus porosity parameters: (a) surface area and (b) porous volume.

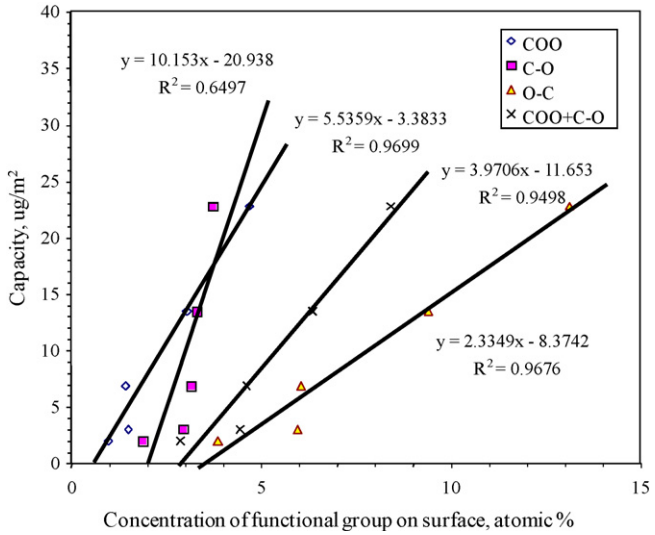

Fig. 9. Capacity per unit area as a function of the group concentration on surface.

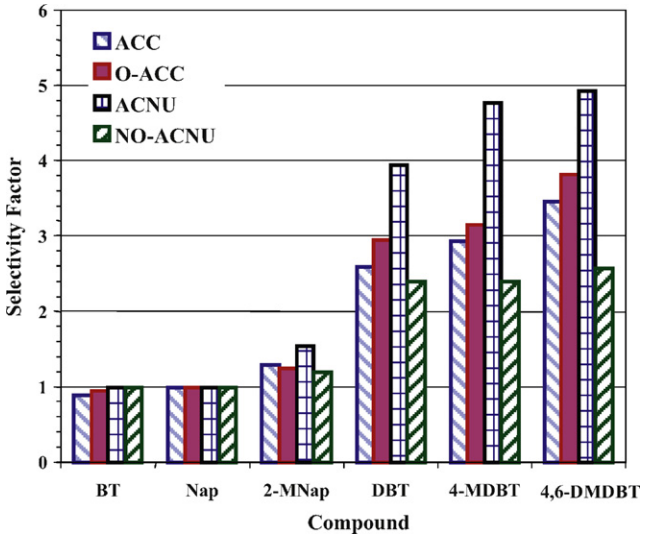

Fig. 10. Adsorption selectivity of ACs for different compounds.

maximum density of the adsorption sites (Q_m) and adsorption equilibrium constant (K). Here, K reflexes the affinity force of the site (chemical property), and Q_m reflexes the density of the potential adsorption sites (the number of function groups per unit area). These three factors work together to determine the adsorption capacity. As Q_m is a linear function of the concentration (C_{fg}) of the related functional groups on the surface ($Q_m = b \cdot C_{fg}$, b is a constant), accordantly the form of Langmuir adsorption isotherm can be changed from:

$$q = \frac{K q_m C}{1 + KC} \tag{4}$$

to

$$\frac{q}{S} = \frac{KC}{1 + KC} b C_{fg} \tag{5}$$

Eq. (5) indicates that the adsorption capacity per unit area (q/S) should have a linear relationship with the concentration (C_{fg}) of the related functional groups on the surface. The adsorption capacities per unit area as a function of the concentration of the related functional groups on the surface are shown in Fig. 9. A good linear relationship was found for CO, COO, O–C and CO+COO functional groups. The adsorption capacity per unit area increased linearly with increasing the oxygen-contained functional groups. These results imply clearly that the oxygen-contained functional groups and their density on the surface play an important role in the adsorption of the sulfur compounds on AC.

3.3.2. Effect on adsorption selectivity

The adsorptive selectivity factors of ACC, O-ACC, ACNU and NO-ACNU for different compounds were calculated and the results are listed in Fig. 10. Interestingly, the adsorptive selectivity factors increase in the order of BT ≈ Nap < 2-MNap < DBT < 4-MDBT < 4,6-DMDBT, regardless the AC samples. As 4,6-DMDBT is a major sulfur compounds remained in the commercial diesel fuel and one of the most refractory sulfur compounds in the commercial diesel, a high adsorptive selectivity of the adsorbent for 4,6-DMDBT is crucial. As shown in Fig. 10, the adsorptive selectivity factor of the tested AC samples for 4,6-DMDBT increases in the order of NO-ACNU < ACC < O-ACC < ACNU, being 2.7, 3.5, 3.8 and 4.9, respectively (see Table 6). The different selectivity factor for 4,6-DMDBT indicates that the adsorbents might have different distribution of the related functional groups on the surface. Some oxygen-containing function group might have higher selectivity for 4,6-DMDBT than others, which will be further explored in our continuous study via computational chemistry approach.

The adsorptive selectivity factors of ACC, O-ACC, ACNU and NO-ACNU for different sulfur compounds versus their total adsorption capacity are shown in Fig. 11. The results show that the selectivity factor for DBTs decreases with increasing total adsorption capacity. For oxidized ACNU, the HNO_3 oxidation enhanced the total adsorption capacity from 3.8 to 11.6 mg-S/g-A, but also resulted in the decrease in the selectivity factor for 4,6-DMDBT from 4.9 to 2.6. Thus, how to increase the total adsorption capacity without loss of the adsorption selectivity for the sulfur compounds is another important issue in development of a novel carbon-based adsorbent.

3.4. Adsorption mechanism

By comparison of the contribution of the different factors to the adsorption capacity in oxidation modification, it appears that

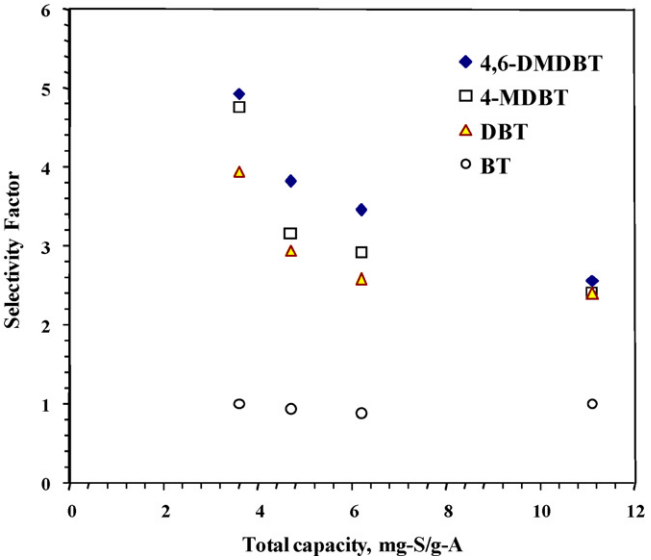

Fig. 11. Adsorption selectivity for different compounds as a function of adsorption capacity.

Table 6
Adsorptive selectivity of ACs for each compound.

Sample	BT	Nap	2-MNap	DBT	4-MDBT	4,6-DMDBT
ACC	0.88	1.00	1.29	2.58	2.92	3.46
O-ACC	0.94	1.00	1.24	2.94	3.15	3.82
ACNU	1.00	1.00	1.54	3.94	4.76	4.92
NO-ACNU	1.00	1.00	1.20	2.40	2.40	2.56

the contribution to the increase in the adsorption capacity is dominantly from the increase in the density (Q_m) of the adsorption sites (oxygen-containing functional groups) and/or *K*-value, but neither from the increase in microporous surface/volume nor from the increase in the mesoporous surface/volume, although Jiang et al. ascribed the contribution of the oxidation modification to the increase in the mesoporous volume [17], and Ania and Bandosz ascribed it partly to the increase in the microporous volume [19]. In fact, the best AC sample, NO-ACNU, has the medium microporous surface/volume in all of the AC samples tested in the present study, as shown in Table 2.

According to the literature, three major adsorption mechanisms have been proposed to explain the adsorption of organic aromatic compounds on AC: the first is the dispersion interaction mechanism, including the π-electron overlap between the adsorbate and the graphene layers (π–π or and π–σ overlap) and the hydrophobic interaction [34–39]. The second is the electron donor–acceptor complex interaction [34,40], including the hydrogen bonding interaction and acid–base interaction. The third is the mechanism of micropore filling combined with adsorption on the "active sites" [19,41].

The adsorption capacity per unit area for the tested AC samples as a function of C-graphite concentration is shown in Fig. 12. It is clear that the adsorption capacity deceases with the increase of C-graphite concentration on the surface. If the adsorption through the π-electron overlap mechanism was the case, the adsorption capacity for sulfur compounds should increase with increasing C-graphite concentration. Therefore, the adsorption through the π-electron overlap mechanism is unlikely. On the other hand, no significant correlation between the adsorption capacity and the micropore surface or micropore volume was observed in the present study (see Fig. 8). The maximum adsorption capacity of the AC samples measured in the present study for the sulfur compounds is about 0.06 ml/g (milliliter of the sulfur compounds per gram of AC), if assuming the average density of the sulfur compounds is 1.1 g/ml. This value is much less than the microporous volume of the ACs (0.085–0.338 ml/g). It indicates that the adsorption for removing the sulfur compounds from liquid hydrocarbon fuel through a micropore filling mechanism is also unlikely. Another argument is that the adsorption of the compounds from liquid hydrocarbon fuel over AC might be governed by the size of molecules, as the adsorptive selectivity for various compounds increases in the order of BT < Nap < 2-MNap < DBT < 4-MDBT < 4,6-DMDBT, as shown in Fig. 10, which is the same as the order of the critical diameter of the molecules (diameter for a largest possible cross-section circle of a molecular conformation [42]) or the area of the molecular plane. Our recent study by using a model fuel containing Nap, 1-MNap, fluorine, DBT, 4,6-DMDBT, indole and quinoline showed that the adsorptive selectivity on the ACs increases in the order of NA < 1-MNA < fluorene < DBT < 4,6-DMDBT < quinoline ≪ indole, although the order of the critical diameter of the molecules (or the area of the molecular plane) increases in the order of indole < NA ≈ quinoline < 1-MNA < DBT ≈ fluorene < 4,6-DMDBT [43]. This result clearly rejects the mechanism of the government by the molecular size.

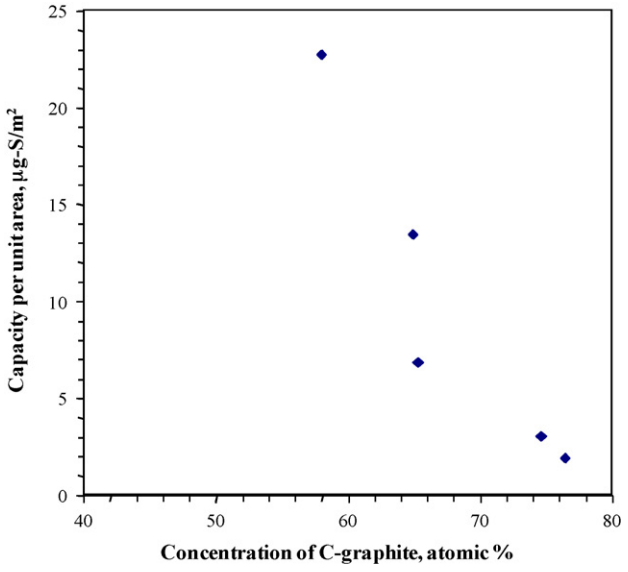

Fig. 12. The adsorption capacity per unit area for the tested AC samples as a function of C-graphite concentration.

All of the findings in the present study suggest that the contribution of the oxidation modification to the improvement in the adsorptive desulfurization performance of AC is through an increase in the oxygen-containing functional groups on the AC surface. Both the excellent correlation observed between the adsorption capacity per unit area and the concentration of the oxygen-containing functional groups, and the good relationship between the adsorption capacities and the pH values support strongly that the adsorption may occur through the interaction of the acidic oxygen-containing groups with thiophenic ring structure or acid–base interaction mechanism. As well known, there are many acidic the oxygen-containing groups on AC surface, including carboxyl, phenol, lactone and lactol groups. Which group on AC surface plays a more important role in adsorption desulfurization and how it interacts with the sulfur compounds are still unclear in the present study. These are being studied in a related work on the basis of the computational chemistry approaches and the characterization of the functional groups by the CO/CO_2 temperature program desorption of AC samples in our laboratory, and the results will be reported in the future.

4. Conclusions

The oxidation modification of AC samples changes their adsorptive desulfurization capacity significantly. The HNO_3 oxidation modification is an efficient modification method in improvement of the adsorptive performance of the AC samples. The improvement extent of the HNO_3 oxidation modification depends also on the initial AC. The adsorptive desulfurization capacity of the HNO_3-oxidized ACNU is about 3.1 times higher than that of the original ACNU, while the adsorptive capacity of the HNO_3-oxidized ACC is about 1.7 times higher than that of the original ACC. The effect of the O_2 oxidation modification at 350–400 °C on the adsorption performance is limited, even negative, depending on the initial AC.

The improvement of the adsorptive performance by the HNO_3 oxidation modification is dominantly through an increase of the oxygen-containing functional groups on the AC surface, but neither through an increase in microporous surface/volume nor through an increase in the mesoporous surface/volume. An excellent correlation between the adsorption capacity per unit area and the

concentration of the oxygen-containing functional groups and a good relationship between the adsorption capacities and the surface pH values suggest that the adsorption of the sulfur compounds on AC may involve an interaction of the acidic oxygen-containing groups with the sulfur compounds.

The adsorptive selectivity factor of the AC samples for different compounds increases in the order of BT $\approx$ Nap $<$ 2-MNap $<$ DBT $<$ 4-MDBT $<$ 4,6-DMDBT, regardless the AC samples. However, the adsorptive selectivity factor decreases with increasing adsorptive capacity in the oxidation modification. Thus, how to increase the total adsorption capacity without loss of the adsorption selectivity for the sulfur compounds is crucial in development of a novel carbon-based adsorbent. Another important issue is the regenerability of the carbon-based adsorbent, which was addressed else [12].

Acknowledgements

This work was supported in part by the U.S. Environmental Protection Agency/National Science Foundation through NSF/EPA TSE Grant No. EPA RD-83147101, by the US Office of Naval Research through its Fuel Cell Program, and by US Department of Energy, National Energy Technology Laboratory through the Refinery Integration project. A. Zhou acknowledges China Scholarship Council for a visiting scholarship during his stay at the Pennsylvania State University.

References

[1] C.S. Song, X.L. Ma, Appl. Catal. B: Environ. 41 (2003) 207–238.
[2] C.S. Song, Catal. Today 86 (2003) 211–263.
[3] X.L. Ma, L. Sun, C.S. Song, Catal. Today 77 (2002) 107–116.
[4] X.L. Ma, M. Sprague, C.S. Song, Ind. End. Chem. Res. 44 (2005) 5768–5775.
[5] A.J. Hernandez-Maldonado, R.T. Yang, Catal. Rev. 46 (2004) 111–1501.
[6] I.V. Babich, J.A. Moulijn, Fuel 82 (2003) 607–631.
[7] S. Murata, K. Murata, K. Kidena, M. Nomura, Energy Fuels 18 (2004) 116–121.
[8] D. Wang, E.W. Qian, H. Amano, K. Okata, A. Ishihara, T. Kabe, Appl. Catal. A: Gen. 253 (2003) 91–99.
[9] K. Kirimura, T. Furuya, R. Sato, Y. Ishii, K. Kino, S. Usami, Appl. Environ. Microbiol. 68 (8) (2002) 3867–3872.
[10] S. Velu, X.L. Ma, C.S. Song, Ind. Eng. Chem. Res. 42 (2003) 5293–5304.
[11] Y. Sano, K.-H. Choi, Y. Korai, I. Mochida, Appl. Catal. B: Environ. 49 (2004) 219–225.
[12] A.N. Zhou, X.L. Ma, C.S. Song, J. Phys. Chem. B 110 (10) (2006) 4699–4707.
[13] A.J. Hernandez-Maldonado, S.D. Stanatis, R.T. Yang, Ind. Eng. Chem. Res. 43 (2004) 769–776.
[14] J.H. Kim, X.L. Ma, A.N. Zhou, C.S. Song, Catal. Today 111 (2006) 74–83.
[15] X.L. Ma, K. Sakanishi, I. Mochida, Ind. Eng. Chem. Res. 33 (1994) 218–222.
[16] T. Garcia, R. Murillo, D. Cazorla-Amoros, A.M. Mastral, A. Linares-Solano, Carbon 42 (2004) 1683–1689.
[17] Z. Jang, Y. Liu, X. Sun, F. Tan, F. Sun, C. Liang, W. You, C. Han, C. Li, Langmuir 19 (2003) 731–736.
[18] S. Haji, C. Erkey, Ind. Eng. Chem. Res. 42 (2003) 6933–6937.
[19] C.O. Ania, T.J. Bandosz, Langmuir 21 (2005) 7752–7759.
[20] C.O. Ania, J.B. Parra, A. Arenillas, F. Rubiera, T.J. Bandosz, J.J. Pis, Appl. Surf. Sci. 253 (2007) 5899–5903.
[21] C. Yu, J.S. Qiu, Y.F. Sun, X.H. Li, G. Chen, Z.B. Zhao, J. Porous Mater. 15 (2008) 151–157.
[22] J.P. Chen, S. Wu, Langmuir 20 (2004) 2233–2242.
[23] A.A. El-Hendawy, Carbon 41 (2003) 713–722.
[24] F. Lopez, F. Medina, M. Prodanov, C. Guell, J. Colloid Interface Sci. 257 (2003) 173–178.
[25] Z.-M. Wang, N. Yamashita, Z.-X. Wang, K. Hoshinoo, H. Kanoh, J. Colloid Interface Sci. 276 (2004) 143–150.
[26] Y. Sano, K.H. Choi, Y. Korai, I. Mochida, Energy Fuels 18 (2004) 644–651.
[27] G. Speranza, N. Laidani, Diamond Relat. Mater. 13 (2004) 445–450.
[28] X.L. Ma, X. Velu, J.H. Kim, C.S. Song, Appl. Catal. B: Environ. 56 (2005) 137–147.
[29] S. Brunauer, L.S. Deming, W.E. Demomg, E. Teller, J. Am. Chem. Soc. 62 (1940) 1723–1732.
[30] S. Biniak, M. Pakula, G.S. Szymaanski, A. Swiatkowski, Langmuir 15 (1999) 6117–6122.
[31] F. Adib, A. Bagreev, T.J. Bandosz, Environ. Sci. Technol. 34 (2000) 636–692.
[32] M.A. Montes-Moran, D. Suarez, J.A. Menendez, E. Fuente, Carbon 42 (2004) 1219–1225.
[33] A.M. Puziy, O.I. Poddubnaya, V.N. Zaitsev, O.P. Konolitska, Appl. Surf. Sci. 221 (2004) 421–429.
[34] C. Moreno-Catilla, Carbon 42 (2004), 83–94.34.
[35] F. Haghseresht, J.J. Funnerty, S. Nouri, G.Q. Lu, Langmuir 18 (2002) 6193–6200.
[36] R.W. Coughlin, F.S. Ezra, Environ. Sci. Technol. 2 (1968) 291.
[37] L.R. Radovic, C. Moreno-Catilla, J. Rivera-Utrilla, Carbon materials as adsorbents in aqueous solutions, in: L.R. Radovic (Ed.), Chemistry and Physics of Carbon, vol. 27, Marcel Dekker, New York, 2000, pp. 227–405.
[38] I. Fleming, Frontier Orbitals and Organic Chemical Reactions, John Wiley and Sons, New York, 1976.
[39] R.G. Barradas, P.G. Hamilton, J. Phys. Chem. 69 (1965) 3411.
[40] J.S. Mattson, H.B.J. Mark, M. Malbin, J. Colloid Interface Sci. 31 (1969) 116.
[41] A.P. Terzyk, J. Colloid Interface Sci. 275 (2004) 9–29.
[42] C.S. Song, X.L. Ma, A.D. Schmitz, H.H. Schobert, Appl. Catal. A: Gen. 182 (1999) 175–181.
[43] M. Almarri, X.L. Ma, C.S. Song, Ind. Eng. Chem. Res., accepted 20 October 2008.